applied optics

Phase correlation during two-photon resonance process in an active cavity

Zifan Zhou,[1,*] Nicholas J. Condon,[3] Devin J. Hileman,[3] Shih C. Tseng,[3] and Selim M. Shahriar[1,2]

[1]Department of Electrical and Computer Engineering, Northwestern University, Evanston, Illinois 60208, USA
[2]Department of Physics and Astronomy, Northwestern University, Evanston, Illinois 60208, USA
[3]Digital Optics Technologies, Rolling Meadows, Illinois 60008, USA
*Corresponding author: zifanzhou2012@u.northwestern.edu

Received 17 October 2019; revised 16 December 2019; accepted 17 December 2019; posted 17 December 2019 (Doc. ID 380614); published 17 January 2020

In this paper, we experimentally demonstrate a strong correlation between the frequencies of the Raman pump and the Raman probe inside an optically pumped Raman laser. We show that the correlation is due to rapid adjustment of the phase of the dipoles that produce the Raman gain, following a sudden jump in the phase of the Raman pump. A detailed numerical model validates this interpretation of the phase correlation. The width of the spectrum of the beat between the Raman pump and the Raman laser is significantly narrowed due to this correlation. As a result, the minimum measurable change in the cavity length, for a given linewidth of the Raman pump laser, is substantially reduced. Therefore, this finding is expected to enhance the sensitivity of such a laser in various metrological applications (e.g., accelerometry).

https://doi.org/10.1364/AO.380614

1. INTRODUCTION

In recent years, we have been investigating superluminal lasers, which can be used for high-precision metrology [1–9]. A superluminal laser is a laser inside which the group velocity of light is much greater than the speed of light in vacuum, without violating causality or special relativity [10]. Such lasers are produced by using a negatively dispersive gain medium with a broad gain profile accompanied by a narrow dip. Previously, we demonstrated a superluminal laser using a diode-pumped alkali laser (DPAL), augmented by a Raman depletion process, with an enhancement factor of ∼190 [8]. However, a DPAL-based superluminal laser is not suitable for some applications that require bi-directional lasing in a single cavity, such as rotation sensing [2]. Therefore, we developed a scheme in which the broad gain profile is produced by the Raman process, corresponding to what is known as a Raman laser [11,12]. Employing this approach, we have recently reported a superluminal Raman laser with an enhancement factor of ∼1080 [13]. In a related work, we also reported earlier a Raman laser with subluminal behavior [14]. The properties of a Raman laser are important in the context of these superluminal and subluminal lasers based on Raman gain. Here, we describe, experimentally as well as theoretically, a property of the Raman laser that was not known previously: the frequency of the Raman laser is highly correlated with that of the Raman pump laser. We also show how this property is expected to lead to enhancement in the sensitivity of sensors, such as an accelerometer. It should be noted that intensity correlations and anticorrelations between two fields applied to a three-level system were observed earlier [15]. However, in that process, the three-level system did not produce a laser field, and no cavity was involved. As such, while somewhat related, the process described here is significantly different from the one reported in Ref. [15].

2. EXPERIMENTAL CONFIGURATION AND RESULTS

The schematic of the experimental apparatus is shown in Fig. 1(a). The cavity is composed of two curved perfect reflectors and a flat output coupler with a reflectivity of ∼90%. One of the curved mirrors is attached to a piezo-electric transducer (PZT). The total length of the cavity is 22.7 cm. The gain medium is a glass cell (5 cm) filled with natural rubidium vapor, which is heated to ∼90°C. However, we only use the ^{85}Rb isotope to produce Raman gain. The Raman pump and the optical pump are combined with a dichroic mirror and then coupled into the cavity using a polarizing beam splitter (PBS). We then use another PBS after the gain cell to extract the pump beams, which is made possible by the fact that the polarizations of the Raman pump and the Raman laser are orthogonal to each other, which are controlled by half-wave plates (HWPs). The power of the optical pump and the Raman pump are 432 mW and 4.2 mW,

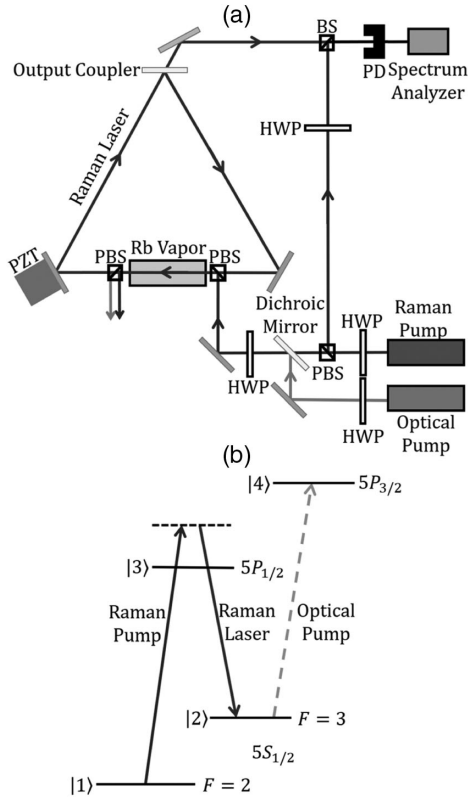

Fig. 1. (a) Schematic of the experiment configuration and (b) relevant energy levels and optical fields in the gain medium.

respectively. To analyze the spectral property of the Raman laser, we take a fraction of the Raman pump and combine it with the output of the Raman laser using a beam splitter (BS). A high-speed photodetector (PD) and a radio-frequency (RF) spectrum analyzer are used to observe the spectrum of the beat signal. Both the Raman pump and the optical pump are distributed Bragg reflector (DBR) diode lasers.

The relevant energy levels and the optical fields are shown in Fig. 1(b). The energy levels are denoted as follows: $|1\rangle \equiv \{5S_{1/2}, F = 2\}$, $|2\rangle \equiv \{5S_{1/2}, F = 3\}$, $|3\rangle \equiv 5P_{1/2}$, and $|4\rangle \equiv 5P_{3/2}$. The optical pump is tuned to the resonance frequency of the $|2\rangle \leftrightarrow |4\rangle$ transition to produce population difference between $|1\rangle$ and $|2\rangle$. The Raman pump is tuned to ∼900 MHz above the resonance frequency of the $|1\rangle \leftrightarrow |3\rangle$ transition. Such a configuration produces a Raman gain along the $|2\rangle \leftrightarrow |3\rangle$ transition, centered at the frequency that, along with the Raman pump, is two-photon resonant for the $|1\rangle \leftrightarrow |2\rangle$ transition.

The power spectra of the beat signals are shown in Fig. 2. Trace C is the beat-note between the Raman laser and the Raman pump, displaying a spectral width of ∼15 kHz. For comparison, the beat-note between the Raman pump laser and a third (reference) DBR laser with nearly identical properties is shown as trace A, which shows a width of ∼1.2 MHz. From this, we can infer that the linewidth of the Raman pump as well as that of the reference DBR laser is ∼0.6 MHz. The beat-note between the Raman laser and the reference DBR laser is shown as trace B, which shows a width of ∼1 MHz, which would imply that the linewidth of the Raman laser is ∼0.4 MHz. As can be seen, the spectral width of the beat-note between the Raman laser and the Raman pump is much less than that of the other two beat-notes. This indicates that there is a strong correlation between the frequencies of the two laser fields involved in the Raman process.

Before proceeding further, we note that we did not have the tools (such as an ultra-narrow laser or an ultra-narrow optical spectral analyzer) to determine the linewidth of any of these three lasers (the Raman pump, the reference DBR, and the Raman laser) independently. Thus, there is a possibility that, in fact, the linewidth of the Raman pump and the Raman laser are closer to each other (each being of the order of ∼0.5 MHz) than what is indicated by the estimates presented above. This would be more consistent with the very narrow spectrum of the beat-note between the Raman laser and the Raman pump.

3. MODELING OF THE FREQUENCY CORRELATION BETWEEN THE RAMAN LASER AND THE RAMAN PUMP

To understand the strong correlation observed between the Raman pump and the Raman laser, we first develop a model in which the frequency of the Raman laser is determined by both the Raman gain profile and the cavity mode profile. Specifically, we make use of the equation of motion for a single-mode laser [16], which shows that the steady-state solution for the Raman laser frequency is determined by the cavity resonance frequency, as modified by the refractive index experienced by the laser field. We consider first the case where the Raman gain is significantly narrower than the cavity mode, corresponding to the conditions used for generating the results shown in Fig. 2. Specifically, the linewidth of the Raman gain is ∼1 MHz [17], and the linewidth of the cavity mode is ∼42 MHz. In Fig. 3(a), we show three Raman gain profiles (shown as A, B, and C) that correspond to three distinct frequencies of the Raman pump. These illustrate the fact that the center of the Raman gain profile shifts with the Raman pump frequency. The cavity mode profile corresponds to the condition when the cavity is empty. In all cases, we define the cavity resonance frequency as F_C, the frequency at which the cavity mode profile is peaked. For the case when the cavity is empty, we define the cavity resonance frequency, F_C, to be F_{REF}. The value of F_{REF} is chosen to be such that when the Raman

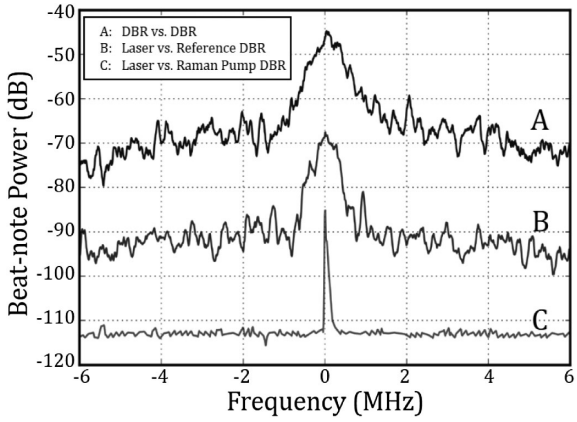

Fig. 2. Experimentally observed phase–noise correlation between the Raman laser and the Raman pump.

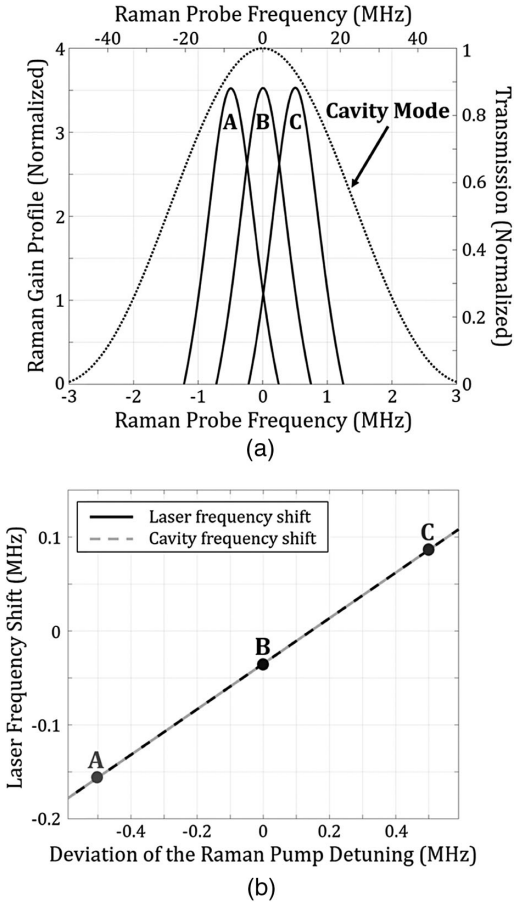

Fig. 3. (a) Schematics of narrow Raman gain profiles (bottom axis and left axis) and the cavity mode (top axis and right axis); (b) the calculated Raman laser frequency shift as a function of the deviation of the Raman pump detuning, away from the reference case corresponding to gain profile B.

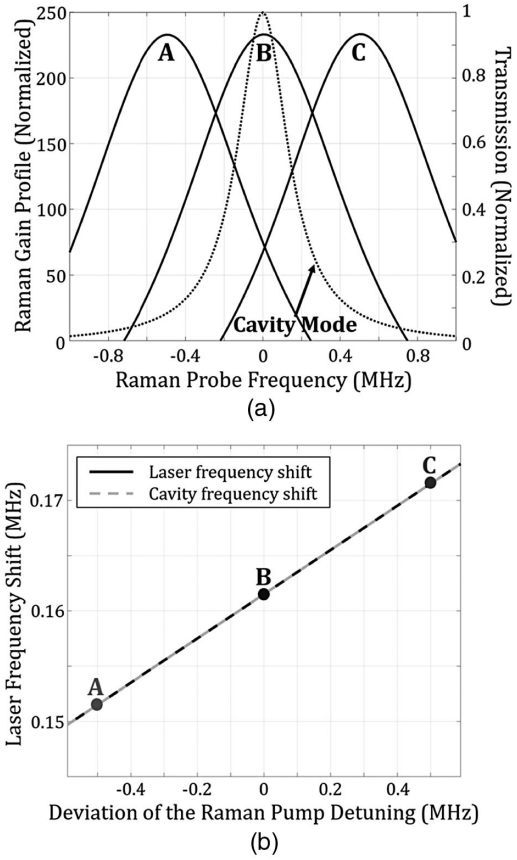

Fig. 4. (a) Schematic of broad Raman gain profiles (left axis) and the cavity mode (right axis); (b) the calculated Raman laser frequency shift as a function of the deviation of the Raman pump detuning away from the reference case corresponding to gain profile B.

pump frequency corresponds to the gain profile B, the difference between the Raman pump frequency and F_{REF} matches the difference between the energies of the two ground states, $|1\rangle$ and $|2\rangle$.

For each gain profile, there is a corresponding dispersion profile. Thus, the peak of the cavity mode (i.e., the value of F_C) is different for each value of the Raman pump detuning. This effect is illustrated by the dashed line in Fig. 3(b), which shows the value of $(F_C - F_{\mathrm{REF}})$ as a function of the deviation of the Raman pump detuning away from the reference case that produces the gain profile B. As can be seen, F_C shifts linearly with the frequency of the Raman pump. Even at the reference condition corresponding to the gain profile B, it should be noted that the value of F_C is slightly different from F_{REF}. This is due to differential light-shifts experienced by the two ground states. The frequency of the Raman laser, for each of the three cases (A, B, and C), is found via numerical simulation to be the same as the cavity resonance frequency, as expected from the single-frequency laser model. This is illustrated by the solid line in Fig. 3(b). The important point to note here is that the Raman laser frequency is correlated with the Raman pump frequency. However, the slope, S, of this correlation line is ~0.25, which is not high enough to explain the data shown in Fig. 2. As shown earlier, the spectral width of the Raman pump laser is ~0.6 MHz. If we use the result of this condition in which the correlation between the Raman pump and the Raman laser is ~0.25, the spectral width of the beat-note between the Raman pump and the Raman laser can be estimated to be $(0.6\ \mathrm{MHz}) \times (1-S) \sim 0.45\ \mathrm{MHz}$, which is much larger than the linewidth of trace C (~15 kHz) in Fig. 2.

To investigate the role of the relative values of the linewidths of the Raman gain and the cavity mode on the amplitude of the correlation slope, we have also considered the complimentary case where the Raman gain profile is broader than the cavity mode, as shown in Fig. 4(a). In Fig. 4(b), we show the shift in the cavity resonance frequency (dashed line) and the shift in the Raman laser frequency (solid line) as functions of the deviation of the Raman pump detuning away from the reference case that produces the gain profile B. Just as in the case of the first condition, the Raman laser frequency is the same as the cavity resonance frequency, as expected. Similarly, just as in the case of the first condition illustrated in Fig. 3, we see that the Raman laser frequency is correlated with the Raman pump frequency. However, in this case, the correlation slope, S, is much smaller, ~0.02. However, in this case the correlation slope (S) is even smaller, ~0.02. Thus, the spectral width of the beat-note between the Raman pump and the Raman laser, under this condition, can be estimated to be

(0.6 MHz) × (1−S) ∼ 0.59 MHz. Again, this is much larger than the linewidth of the trace C (∼15 kHz) in Fig. 2. Thus, we conclude that the shift in the cavity resonance frequency is not adequate enough to explain the strong degree of frequency correlation found experimentally.

In the results we have shown in Figs. 3 and 4, we have employed the steady-state solutions of the laser equation. To explore additional factors that produce the strong frequency correlations, it is necessary to consider the gain process dynamically, as shown in the next section.

4. DYNAMIC MODELING OF THE PHASE–NOISE CORRELATION

The linewidth of a continuous wave laser can be modeled as being due to random jumps in its phase [16]. The amount of phase change in each jump, and how often these jumps occur, together determine the linewidth. This process is illustrated schematically in Fig. 5(a) for the Raman pump. The observed condition, as shown in Fig. 2, indicates that these jumps cause corresponding changes in the phase of the Raman laser, as illustrated qualitatively in Fig. 5(b). The goal of the model described below is to determine the manner in which the Raman laser phase may be affected by a jump in the phase of the Raman laser, and the resulting degree of correlation.

We consider the gain medium (^{85}Rb) to be a three-level system, as shown in Fig. 6. The relevant energy levels are denoted as follows: $|1\rangle \equiv \{5S_{1/2},\ F=2\}$, $|2\rangle \equiv \{5S_{1/2},\ F=3\}$, and $|3\rangle \equiv 5P_{1/2}$. The Raman pump is tuned above the $|1\rangle \leftrightarrow |3\rangle$ transition by an amount δ_{RP}. The Raman laser field is tuned above the $|2\rangle \leftrightarrow |3\rangle$ transition by an amount δ_{RL}. For simplicity, we assume that the rate of decay from $5P_{1/2}$ to $5S_{1/2}$, $F=2$ and $5S_{1/2}$, $F=3$ are equal, indicated as $\Gamma/2$ in Fig. 6. We also assume collisional decay rates from $|1\rangle$ to $|2\rangle$ (γ_{12}) and $|2\rangle$ to $|1\rangle$ (γ_{21}) to be equal. The optical pump is modeled as an effective decay from $|2\rangle$ to $|1\rangle$, which is denoted as Γ_{OP} in the schematic.

The Hamiltonian of such a system after applying rotating wave approximation can be written as

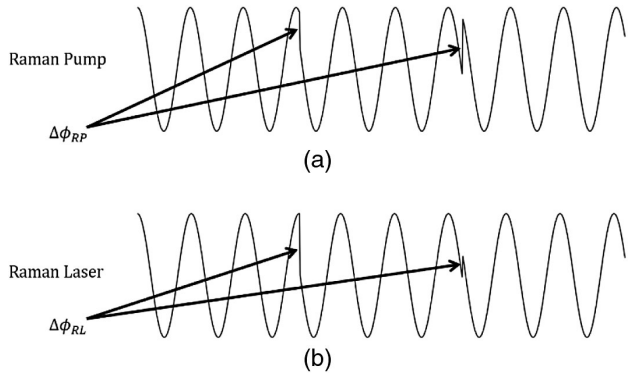

Fig. 5. (a) Schematic of illustration of a random phase jump $\Delta\phi_{\mathrm{RP}}$ introduced for the Raman pump. (b) Schematic illustration of the corresponding phase jump $\Delta\phi_{\mathrm{RL}}$ that may be experienced by the Raman laser.

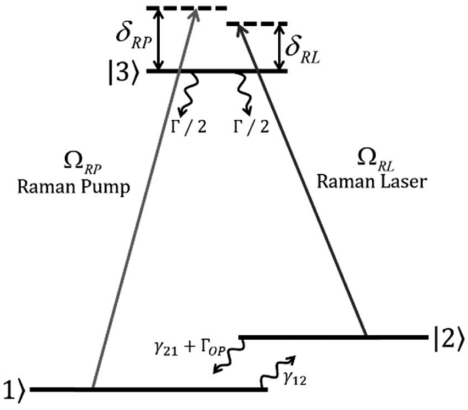

Fig. 6. Relevant energy levels, optical fields, and decay rates in the gain medium.

$$H/\hbar = \begin{bmatrix} \omega_1 & 0 & \frac{\Omega_{\mathrm{RP}}}{2} e^{i(\omega_{\mathrm{RP}} t+\phi_{\mathrm{RP}})} \\ 0 & \omega_2 & \frac{\Omega_{\mathrm{RL}}}{2} e^{i(\omega_{\mathrm{RL}} t+\phi_{\mathrm{RL}})} \\ \frac{\Omega_{\mathrm{RP}}}{2} e^{-i(\omega_{\mathrm{RP}} t+\phi_{\mathrm{RP}})} & \frac{\Omega_{\mathrm{RL}}}{2} e^{-i(\omega_{\mathrm{RL}} t+\phi_{\mathrm{RL}})} & \omega_3 \end{bmatrix}. \tag{1}$$

Here, $\hbar\omega_j\,(j=1,2,3)$ is the energy of the state $|j\rangle$, $\Omega_{\mathrm{RP}}(\Omega_{\mathrm{RL}})$ is the Rabi frequency for the Raman pump (Raman laser), ω_{RP} (ω_{RL}) is the angular frequency of the Raman pump (Raman laser), and ϕ_{RP} (ϕ_{RL}) is the phase of the Raman pump (Raman laser). To eliminate the time dependence of the Hamiltonian as well as the phases in the off-diagonal terms, we first carry out a rotating wave transformation, under which the quantum state $|\psi\rangle$ is transformed to $|\tilde{\psi}\rangle$ as follows:

$$|\tilde{\psi}\rangle \equiv Q_1|\psi\rangle, \tag{2}$$

where Q_1 is defined as

$$Q_1 \equiv e^{-i(\theta_1 t+\eta_1)}\,|1\rangle\langle 1| + e^{-i(\theta_2 t+\eta_2)}\,|2\rangle\langle 2| + e^{-i(\theta_3 t+\eta_3)}\,|3\rangle\langle 3|, \tag{3}$$

with $\theta_1=\omega_1$, $\eta_1=\phi_{\mathrm{RP}}$, $\theta_2=\omega_2+\delta_{\mathrm{RP}}-\delta_{\mathrm{RL}}$, $\eta_2=\phi_{\mathrm{RL}}$, $\theta_3=\omega_3+\delta_{\mathrm{RP}}$, and $\eta_3=0$. We define a matrix M such that $dQ_1/dt = iMQ_1$, so that

$$M=\theta_1|1\rangle\langle 1|+\theta_2|2\rangle\langle 2|+\theta_3|3\rangle\langle 3|. \tag{4}$$

The effective Hamiltonian [18] then becomes $\tilde{H} = Q_1 H Q_1^{-1} - \hbar M$:

$$\tilde{H}/\hbar = \begin{bmatrix} 0 & 0 & \Omega_{\mathrm{RP}}/2 \\ 0 & -\delta_{\mathrm{RP}}+\delta_{\mathrm{RL}} & \Omega_{\mathrm{RL}}/2 \\ \Omega_{\mathrm{RP}}/2 & \Omega_{\mathrm{RL}}/2 & -\delta_{\mathrm{RP}} \end{bmatrix}. \tag{5}$$

The atomic decay and collisional decays can be taken into account by adding complex terms to the Hamiltonian:

$$\tilde{H}/\hbar = \begin{bmatrix} -i\frac{\gamma_{12}}{2} & 0 & \frac{\Omega_{\mathrm{RP}}}{2} \\ 0 & -\delta_{\mathrm{RP}}+\delta_{\mathrm{RL}}-i\frac{\gamma_{21}+\Gamma_{\mathrm{OP}}}{2} & \frac{\Omega_{\mathrm{RL}}}{2} \\ \frac{\Omega_{\mathrm{RP}}}{2} & \frac{\Omega_{\mathrm{RL}}}{2} & -\delta_{\mathrm{RP}}-i\frac{\Gamma}{2} \end{bmatrix}. \tag{6}$$

In terms of this Hamiltonian, the equation of motion can be expressed as the Liouville equation:

$$\dot{\tilde{\rho}} = -\frac{i}{\hbar}[\tilde{H}\tilde{\rho} - \tilde{\rho}\tilde{H}^*] + \frac{\partial}{\partial t}\tilde{\rho}_{\text{source}}, \tag{7}$$

$$\frac{\partial}{\partial t}\tilde{\rho}_{\text{source}} = \left[(\gamma_{21} + \Gamma_{\text{OP}})\,\tilde{\rho}_{22} + (\Gamma/2)\,\tilde{\rho}_{33}\right]|1\rangle\langle 1| + \left[\gamma_{12}\tilde{\rho}_{11} + (\Gamma/2)\,\tilde{\rho}_{33}\right]|2\rangle\langle 2|, \tag{8}$$

where $\tilde{\rho}$ is the density matrix. We use the steady-state solution of this equation as the initial conditions for the subsequent modeling of the effect of the phase jump.

We introduce a phase jump $\Delta\phi_{\text{RP}}$ in the Raman pump. The phase of the Raman laser is changed by an amount $\Delta\phi_{\text{RL}}$, which is to be determined. The value of the phase jump $\Delta\phi_{\text{RL}}$ can be established by requiring [19] that it would maximize the gain experienced by the Raman laser, which is proportional to the imaginary part of the term $\tilde{\rho}_{23}$ of the density matrix. We first apply a transformation to the Hamiltonian to find the susceptibility experienced by the Raman laser field after the Raman pump phase jump occurs. Since the phases of the Raman pump and the Raman laser have changed, the values of η_1 and η_2 in the Q_1 matrix of Eq. (3) should be updated accordingly. This can be accomplished by simply carrying out an additional transformation with a matrix Q_2 so that $\tilde{\tilde{H}} = Q_2\tilde{H}Q_2^{-1}$, where Q_2 is defined as

$$Q_2 = e^{-i\Delta\phi_{\text{RP}}}|1\rangle\langle 1| + e^{-i\Delta\phi_{\text{RL}}}|2\rangle\langle 2| + |3\rangle\langle 3|. \tag{9}$$

The resulting complex Hamiltonian can be expressed as

$$\tilde{\tilde{H}}/\hbar = \begin{bmatrix} -i\frac{\gamma_{12}}{2} & 0 & \frac{\Omega_{\text{RP}}}{2}e^{-i\Delta\phi_{\text{RP}}} \\ 0 & \delta_{\text{RL}} - \delta_{\text{RP}} - i\frac{\gamma_{21}+\Gamma_{\text{OP}}}{2} & \frac{\Omega_{\text{RL}}}{2}e^{-i\Delta\phi_{\text{RL}}} \\ \frac{\Omega_{\text{RP}}}{2}e^{i\Delta\phi_{\text{RP}}} & \frac{\Omega_{\text{RL}}}{2}e^{i\Delta\phi_{\text{RL}}} & -\delta_{\text{RP}} - i\frac{\Gamma}{2} \end{bmatrix}. \tag{10}$$

For a specific set of $\Delta\phi_{\text{RP}}$ and $\Delta\phi_{\text{RL}}$, by evolving the density matrix using the Liouville equations, we can find the gain in the Raman laser as a function of time, which starts oscillating after introducing a phase jump, as illustrated in Fig. 7(a). Eventually, the density matrix reaches steady state again, and it is identical to the solution before adding phase jumps in the system, as shown in Fig. 7(b). Before reaching steady state, the mean value of the imaginary part of $\tilde{\rho}_{23}$ (the gain in the Raman laser) also oscillates, as shown in Fig. 7(c). The solid line in Fig. 7(c) is calculated by averaging the imaginary part of $\tilde{\rho}_{23}$ over 25 ns. For a given $\Delta\phi_{\text{RP}}$, the gain experienced by the Raman laser before reaching steady state varies as a function of $\Delta\phi_{\text{RL}}$. For example, consider the gain at time t_A in Fig. 7(c). This value corresponds to the condition where $\Delta\phi_{\text{RP}} = \Delta\phi_{\text{RL}} = -\pi/4$. If we now vary $\Delta\phi_{\text{RL}}$, the gain at time t_A will vary. This is illustrated in Fig. 8(a). As can be seen, for $\Delta\phi_{\text{RP}} = \Delta\phi_{\text{RL}}$ (indicated by the vertical dashed line), the gain has the maximum value, which is the same as the value shown in Fig. 7(c) at time t_A. When the value of $\Delta\phi_{\text{RL}}$ is scanned around this point, it always decreases. The same behavior is observed (not shown) at any other time point (such as t_B and t_C) in Fig. 7(c). Thus, we conclude that the transient value of the locally averaged (over 25 ns) gain is always maximized when $\Delta\phi_{\text{RP}} = \Delta\phi_{\text{RL}}$. We have confirmed the same

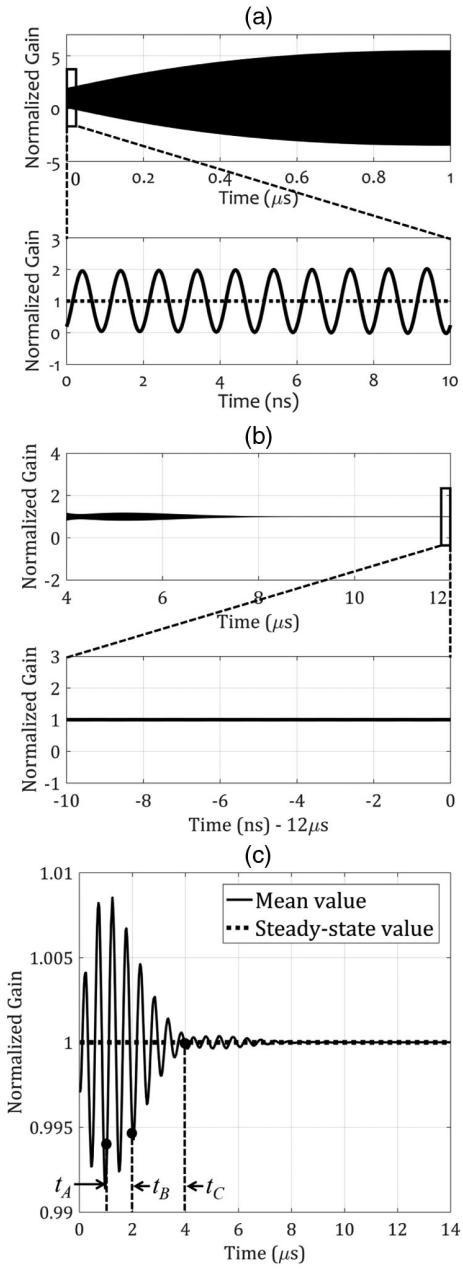

Fig. 7. Normalized gain as functions of time for (a) a short period of time after introducing a phase jump, (b) approaching steady state. (c) The mean value of the normalized gain over a short period of time as a function of time. The figures are generated using $\Delta\phi_{\text{RP}} = \Delta\phi_{\text{RL}} = -\pi/4$.

behavior at other values of $\Delta\phi_{\text{RP}}$, as illustrated in Figs. 8(b)–8(d). In each of these cases, we see that the peak gain occurs when $\Delta\phi_{\text{RP}} = \Delta\phi_{\text{RL}}$, as indicated by the vertical dashed lines.

In Fig. 9, we show the deviation of the Raman laser frequency as a function of the deviation of the Raman pump detuning away from the reference point for different models, as well as the result inferred from the experimental data. Line A and Line B are reproductions of the results shown in Figs. 3(b) and 4(b), respectively. Line C is the result concluded from the model presented in this section. If we use the observed linewidth (~15 kHz) to calculate the corresponding slope, we find S to

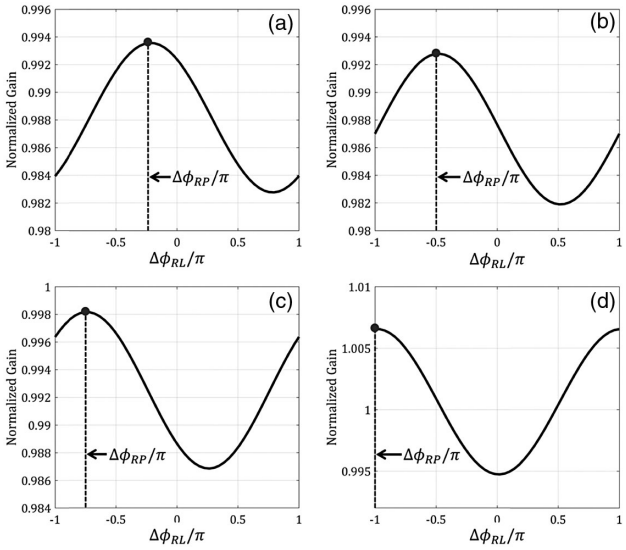

Fig. 8. (a) Normalized gain at $T_{\text{total}} = t_A$ of Fig. 7(c), as a function of $\Delta\phi_{\text{RL}}$, with $\Delta\phi_{\text{RP}}$ fixed at $-\pi/4$. (b), (c), and (d) Similar variations in gain, at a fixed T_{total}, as functions of $\Delta\phi_{\text{RL}}$, for three other fixed values of $\Delta\phi_{\text{RP}}$: $-\pi/2$, $-3\pi/4$, and $-\pi$, respectively.

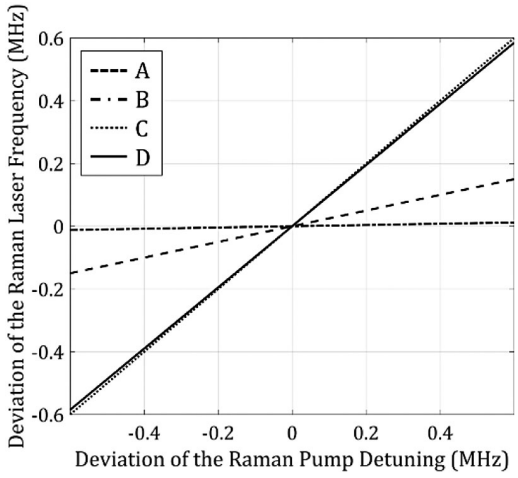

Fig. 9. Deviation of the Raman laser frequency as functions of the deviation of the Raman pump detuning away from the reference frequency.

be $(1-15\,\text{kHz}/0.6\,\text{MHz}) \sim 0.975$, which is shown as Line D in Fig. 9. As can be seen, the slope of Line C is approaching the slope of Line D, with a 2.5% difference. We can thus infer that this model explains well the strong correlation between the Raman laser and the Raman pump.

5. REQUIREMENT OF SPECTRAL CHARACTERISTIC FOR THE RAMAN PUMP EMPLOYED FOR SENSING APPLICATIONS

As noted earlier, a superluminal ring laser (SRL) employing the Raman gain and Raman depletion processes, as described in Refs. [13,14], can be used to measure the change in the cavity length with extremely high sensitivity. When such a system is used for measuring rotation rates, the signal is measured by monitoring the beat frequency between two counter-propagating SRLs, so that all common mode jitters due to excess noise are cancelled out, and the sensitivity is determined by the quantum-noise-limited linewidths of the SRLs only. However, when such a device is used for measuring an unidirectional effect, such as acceleration (with one of the cavity mirrors mounted on a metallic diaphragm, which acts as a transducer, for example), the signal is measured by monitoring the beat frequency between an unidirectional SRL, and a reference laser. A convenient choice for the reference laser is the Raman pump used for producing the Raman gain for the SRL (note that the Raman pump used for producing the Raman depletion is offset phase locked to the Raman pump used for producing the Raman gain). Under this scenario, the linewidth of the Raman gain pump and the correlation between the Raman gain pump and the Raman laser (which is the SRL) together determine the effective linewidth of the beat frequency, assuming that this is much larger than the quantum-noise-limited linewidth of the Raman gain pump and that of the SRL. In what follows, we carry out a quantitative analysis, showing how the correlation presented in Fig. 2 enhances the sensitivity of such a measurement significantly, for a given linewidth of the Raman gain pump.

For a given acceleration rate A, the laser frequency shift, f_A (in Hz), can be expressed as

$$f_A = \xi \cdot \Sigma \cdot A, \tag{11}$$

where, ξ is the superluminal enhancement factor, and Σ is the scale factor, which is determined by the parameters of the cavity and the transducer. Here, we assume the transducer to be a MEMS (micro electro-mechanical system)-based mirror, suspended on a spring-like structure. Then the scale factor can be written as

$$\Sigma = \left(\frac{m}{k}\right) \frac{2c}{L\lambda \cos(\theta/2)}, \tag{12}$$

where, m is the mass of the MEMS mirror, k is the spring constant of the MEMS support, c is the speed of light in vacuum, L is the perimeter of the laser, λ is the laser wavelength, and θ is the full-angle of the cavity mode at the MEMS mirror. We denote as Γ_{RP} the linewidth of the Raman pump and assume that it is much larger than its quantum-noise-limited linewidth. Similarly, we denote as γ_{RL} the linewidth of the Raman laser and assume that it is much larger that its quantum-noise-limited linewidth. Then, in the absence of any correlation between the frequencies of the Raman pump and the Raman laser, the linewidth of the beat-note is expected to be approximately $(\Gamma_{\text{RP}} + \gamma_{\text{RL}})$. However, as we have shown in Fig. 2, there is a strong correlation between the frequencies of the Raman pump and the Raman laser. Let us denote the effective correlation factor as ζ, defined so that the spectral width of the beat-note can be expressed as $\Delta f_A = \Gamma_{\text{RP}}/\zeta$. The minimum measurable acceleration (MMA), A_{min}, can be then expressed as

$$A_{\text{min}} = \frac{1}{\xi\Sigma}\Delta f_A = \frac{1}{\xi\Sigma}\frac{\Gamma_{\text{RP}}/\zeta}{\eta}, \tag{13}$$

where η is a dimensionless number representing the signal-to-noise ratio (SNR), which depends on the integration time. Here we define η_0 as the SNR for an integration time of 1 second. Then we can express Eq. (13) as

$$A_{\min} = \frac{1}{\xi \Sigma} \Delta f_A = \frac{1}{\xi \zeta \Sigma} \frac{\Gamma_{\mathrm{RP}}}{\eta_0 \sqrt{\tau}}, \tag{14}$$

where τ is a dimensionless number, given by the integration time divided by 1 second. The value of η_0 is given by the square-root of the number of photons falling on the beat detector in 1 second. If we denote the quantum efficiency of the detection process as ρ, and denote the power of the SRL output as P (in watts), we can find

$$\eta_0 = \sqrt{\rho P / (\hbar \omega_0)}, \tag{15}$$

where ω_0 is the frequency of the Raman pump (in rad/s). By combining Eqs. (14) and (15), we can express the Raman pump linewidth as

$$\Gamma_{\mathrm{RP}} = A_{\min} \xi \zeta \Sigma \sqrt{\rho P / (\gamma_B \hbar \omega_0)}, \tag{16}$$

where γ_B is defined as the dimensionless operating bandwidth, $\gamma_B \equiv 1/\tau$. Based on a typical MEMS-based transducer, we consider, for example, the value of $\Sigma\Sigma$ to be 4×10^6 Hz/g, where g is the gravitational acceleration. For the data shown in Fig. 2, we determined the value of ζ to be $\sim$25. For an SRL output power of 1 μW, and $\rho = 0.25$, we find $\eta_0 \simeq 1.4 \times 10^6$. If we choose the operating bandwidth γ_B to be 10^3, corresponding to a detection bandwidth of 1 kHz, for MMA of 1 pico $-$ g (10^{-12}g), the maximum spectral width of the Raman pump is $\sim$320 kHz, which is not a very challenging requirement for a typical diode laser.

6. SUMMARY

To summarize, we have experimentally demonstrated a strong correlation between the frequencies of the Raman pump and the Raman probe inside an optically pumped Raman laser. We have also shown that the correlation is due to rapid adjustment of the phase of the dipoles that produce the Raman gain following a sudden jump in the phase of the Raman pump. We have described the results of a detailed numerical model that validates this interpretation of the phase correlation. Since the width of the spectrum of the beat between the Raman pump and the Raman laser is significantly narrowed as a result of this correlation, the minimum measurable change in the cavity length, for a given linewidth of the Raman pump laser, is substantially reduced. Therefore, this finding is expected to enhance the sensitivity of such a laser in various metrological applications (e.g. accelerometry).

Funding. Air Force Office of Scientific Research (FA9550-18-01-0401, FA9550-18-P-0003); National Aeronautics and Space Administration (80NSSC18P2077); Defense Security Cooperation Agency (PO4440778007).

Disclosures. The authors declare no conflict of interest.

REFERENCES AND NOTES

1. H. N. Yum, M. Salit, J. Yablon, K. Salit, Y. Wang, and M. S. Shahriar, "Superluminal ring laser for hypersensitive sensing," Opt. Express **18**, 17658–17665 (2010).
2. M. S. Shahriar, G. S. Pati, R. Tripathi, V. Gopal, M. Messall, and K. Salit, "Ultrahigh enhancement in absolute and relative rotation sensing using fast and slow light," Phys. Rev. A **75**, 1–10 (2007).
3. G. S. Pati, M. Salit, K. Salit, and M. S. Shahriar, "Demonstration of displacement-measurement-sensitivity proportional to inverse group index of intra-cavity medium in a ring resonator," Opt. Commun. **281**, 4931–4935 (2008).
4. D. D. Smith, H. Chang, L. Arissian, and J. C. Diels, "Dispersion-enhanced laser gyroscope," Phys. Rev. A **78**, 1–9 (2008).
5. J. Scheuer and S. M. Shahriar, "Lasing dynamics of super and sub luminal lasers," Opt. Express **23**, 32350–32366 (2015).
6. O. Kotlicki, J. Scheuer, and M. S. Shahriar, "Theoretical study on Brillouin fiber laser sensor based on white light cavity," Opt. Express **20**, 28234–28248 (2012).
7. H. N. Yum and M. S. Shahriar, "Pump-probe model for the Kramers-Kronig relations in a laser," J. Opt. **12**, 104018 (2010).
8. J. Yablon, Z. Zhou, M. Zhou, Y. Wang, S. Tseng, and M. S. Shahriar, "Theoretical modeling and experimental demonstration of Raman probe induced spectral dip for realizing a superluminal laser," Opt. Express **24**, 27444–27456 (2016).
9. D. T. Kutzke, O. Wolfe, S. M. Rochester, D. Budker, I. Novikova, and E. Mikhailov, "Tailorable dispersion in a four-wave mixing laser," Opt. Lett. **42**, 2846–2849 (2017).
10. L. J. Wang, A. Kuzmich, and A. Dogariu, "Gain-assisted superluminal light propagation," Nature **406**, 277–279 (2000).
11. P. Kumar and J. H. Shapiro, "Observation of Raman-shifted oscillation near the sodium D lines," Opt. Lett. **10**, 226–228 (2008).
12. M. Poelker and P. Kumar, "Sodium Raman laser: direct measurements of the narrow-band Raman gain," Opt. Lett. **17**, 399–401 (2008).
13. Z. Zhou, M. Zhou, and S. M. Shahriar, "A superluminal Raman laser with enhanced cavity length sensitivity," Opt. Express **27**, 29738–29745 (2019).
14. J. Yablon, Z. Zhou, N. Condon, D. Hileman, S. Tseng, and S. Shahriar, "Demonstration of a highly subluminal laser with suppression of cavity length sensitivity by nearly three orders of magnitude," Opt. Express **25**, 30327–30335 (2017).
15. V. A. Sautenkov, Y. V. Rostovtsev, and M. O. Scully, "Switching between photon-photon correlations and Raman anticorrelations in a coherently prepared Rb vapor," Phys. Rev. A **72**, 065801 (2005).
16. M. Sargent, M. Scully, and W. Lamb, *Laser Physics*, 1st ed. (CRC Press, 1974).
17. G. S. Pati, M. Salit, K. Salit, and M. S. Shahriar, "Simultaneous slow and fast light effects using probe gain and pump depletion via Raman gain in atomic vapor," Opt. Express **17**, 8775–8780 (2009).
18. M. S. Shahriar, Y. Wang, S. Krishnamurthy, Y. Tu, G. S. Pati, and S. Tseng, "Evolution of an N-level system via automated vectorization of the Liouville equations and application to optically controlled polarization rotation," J. Mod. Opt. **61**, 351–367 (2014).
19. This is analogous to what happens in a laser when the cavity length changes slightly while the laser is in steady state. The lasing wavelength moves to the one that is resonant with the new length of the cavity, since this new wavelength experiences less loss than the original one. In the current case, the phase of the Raman laser moves to a new value that sees more gain than the original one.